Damping of a micro-resonator torsion mirror in rarefied gas ambient

2005 J. Micromech. Microeng. 15 1762

(http://iopscience.iop.org/0960-1317/15/9/019)

INSTITUTE OF PHYSICS PUBLISHING JOURNAL OF MICROMECHANICS AND MICROENGINEERING

J. Micromech. Microeng. **15** (2005) 1762–1769 doi:10.1088/0960-1317/15/9/019

Damping of a micro-resonator torsion mirror in rarefied gas ambient

Adi Minikes[1], **Izhak Bucher**[2] **and Gal Avivi**[1]

[1] Dynamics Laboratory, Faculty of Mechanical Engineering Technion, Israel Institute of Technology, Haifa 3200, Israel
[2] Head of Dynamics Laboratory, Faculty of Mechanical Engineering Technion, Israel Institute of Technology, Haifa 3200, Israel

E-mail: minikes@technion.ac.il, bucher@technion.ac.il and agal@technion.ac.il

Received 3 March 2005, in final form 25 May 2005
Published 21 July 2005
Online at stacks.iop.org/JMM/15/1762

Abstract
Damping in resonating MEMS mirrors has a profound effect on the dynamical behavior. The validity of the existing theories is investigated in this work by theoretical and experimental means. The squeeze-film model with artificial viscosity and the molecular dynamics model are adapted for the case of a torsion mirror under a wide range of vacuum levels. The considered ambient pressure varies from atmospheric to a pressure under which structural damping prevails. High resolution experiments have been conducted on dedicated devices. Two independent experimental damping extraction methods have been employed for substantiating the validity of the measured parameters. Although the theoretical models agree favorably with the experimental data, it appears they provide slightly different predictions under different operating regimes.

1. Introduction

An electrostatic torsion mirror is characterized by a planar micro-machined surface tilting harmonically in close proximity to fixed electrodes in the substrate. Designed for high electrostatic actuation efficiency, the gap between the elements is about two to three orders of magnitude smaller than the characteristic length of the mirror and is typically only a few micrometers. In the presence of gas, engulfing the microstructure, the damping effects are dominated by the squeeze-film phenomenon which deteriorates the torsion mirror performance in terms of sensitivity and resolution. Operating in rarefied gas ambient reduces the energy losses in the system, hence, increasing the quality factor of the mechanical vibrating device.

Currently, there are two approaches for modeling the damping mechanism of micro resonators in rare gas ambient. One approach, presented by Veijola *et al* [1] and Li and Hughes [2], suggests an 'effective coefficient of viscosity' in which an approximated viscosity coefficient depends on the gas pressure via the Knudsen number of the system. Solving the Reynolds equation which governs the squeeze-film damping phenomenon and utilizing this empirical coefficient in the solution allow the prediction of the damping effect for different ambient pressures. The concept of equivalent viscosity loses its physical meaning in rarefied environment since the molecules' collisions with each other are so rare that the gas can no longer be considered as a continuum.

An alternative approach presented by Christian [3], Bao *et al* [4] and Hutcherson and Ye [5] is based on free molecular dynamic models developed for a plate vibrating in normal direction to a nearby stationary wall. The model originally derived by Christian [3] is based on momentum transfer rate from the vibrating plate to the surrounding gas due to collisions of molecules with the plate. His model does not incorporate the effects caused by the presence of a nearby wall and the quality factor is independent of the dimensions of the oscillating surface. A more accurate model for predicating the quality factor when the vibrating plate is not isolated was suggested by Bao *et al* [4]. This model is based on energy transfer and on the velocity change of gas molecules due to collision with the vibrating surface. Bao *et al* [4] have shown that for an oscillating plate near a wall, the quality factor obtained by the energy transfer model is about one order of magnitude smaller than that obtained by the Christian model. Hutcherson and Ye [5] have further modified Bao's model by removing the assumption of constant particle velocity while a molecule is traveling underneath the oscillating plate, thus reducing the

underestimation of the energy transferred to the gas. This modified model is implemented numerically, and therefore it loses some of its appeal as an engineering design tool.

Recently, much interest in the dynamical behavior of a micro-machined torsion mirror and the effect of damping has risen due to its wide technological impact. Pan *et al* [6] have solved a linearized Reynolds equation to obtain the damping torque on a tilting mirror by means of Fourier and double sine series. Although the obtained solutions include both spring forces and viscous forces induced by the squeezed film, only cases with small squeeze numbers (viscous forces, see [11]) are valid. At high squeeze numbers, nonlinear effects become significant, making the linearized Reynolds equation rather inaccurate [7]. Pan *et al* [6] have investigated the dynamical behavior of a tilting mirror in atmospheric pressure only and verified the results experimentally. A numerical damping model for a two-dimensional octagonal gimbaled tilting mirror was introduced by Hao *et al* [8]. Their paper begins by presenting an analytical solution for a 1D tilting mirror obtained by solving a variant of the linearized Reynolds equation, but apparently the provided expression is identically zero and the suitability of the solution was not verified. A different approach to reduce the damping force generated by the squeeze film was introduced by Uchida *et al* [9] who have fabricated deep grooves in the electrodes. The presence of grooves reduces the damping moment but at the same time decreases the electrostatic driving force.

In this paper, an analytical and experimental study on the damping effects of a rectangular torsion mirror as a function of the ambient pressure has been carried out. First, an analytical expression for the squeeze-film damping coefficient in a tilting mirror is derived. This solution is obtained by degenerating the Reynolds equation into a Poisson's equation, considering viscous damping effects only. Next, the free molecular model given by Bao *et al* [4] is utilized for the case of a mirror exhibiting an angular motion. An experimental study on a dedicated micro-resonator torsion mirror concludes the paper, comparing and validating the agreements of the theoretical models.

2. Squeeze-film model

A rectangular 1D oscillating torsion mirror is illustrated schematically in figure 1. The mirror is assumed to be perfectly rigid and tilts around the y axis by a small angle $\theta \ll 1$. The initial gap between the mirror and the substrate is given by $h_0 \ll a$. At ambient pressure, where the Knudsen number is relatively small and the engulfing gas could be considered as continuum flow, the dominating damping mechanism is the squeeze film underneath the mirror. The viscous forces in the layer reach equilibrium with the pressure forces and the damping torque results forming the spatial pressure distribution in the film.

The governing equation is the Reynolds equation derived from Navier–Stokes equations with non-slip boundary conditions. The nonlinear and isothermal Reynolds equation in rectangular coordinates and in non-dimensional form is given by Langlois [10]:

$$\frac{\partial}{\partial X}\left(H^3 P \frac{\partial P}{\partial X}\right) + \frac{\partial}{\partial Y}\left(H^3 P \frac{\partial P}{\partial Y}\right) = \sigma \frac{\partial (PH)}{\partial \tau}, \qquad (1)$$

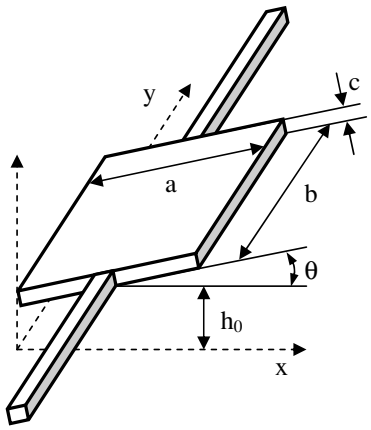

Figure 1. Schematic layout of the torsion mirror actuator.

where the non-dimensional parameters are

$$P = \frac{p}{p_0}, \qquad H = \frac{h}{h_0}, \qquad X = \frac{x}{a},$$
$$Y = \frac{y}{a}, \qquad \tau = \omega t, \qquad \sigma = \frac{12\mu\omega a^2}{p_0 h_0^2}, \qquad (2)$$

where p_0 and μ represent the surrounding gas pressure and the gas viscosity, respectively. The vibrating frequency of the mirror is given by ω and the squeeze number σ is related to the energetic level of the film. At low squeeze numbers, the compressibility effects in the squeeze film are negligible and the film acts as a dashpot, while at high squeeze numbers the film behaves as a nonlinear spring, exhibiting little dissipation [11, 12].

Assuming pressure release boundary conditions:

$$P(0, Y, \tau) = P(1, Y, \tau) = P(X, 0, \tau) = P(X, b/a, \tau) = 1. \qquad (3)$$

Under small amplitudes of the mirror's angular motion, the pressure and the clearance could be represented by introducing a small perturbation parameter such as

$$H = 1 + \delta \tilde{H}, \qquad P = 1 + \delta \tilde{P}. \qquad (4)$$

Substituting these forms into the Reynolds equation and collecting only first-order terms result in a linearized Reynolds equation:

$$\frac{\partial^2 \tilde{P}}{\partial X^2} + \frac{\partial^2 \tilde{P}}{\partial Y^2} = \sigma\left(\frac{\partial \tilde{P}}{\partial \tau} + \frac{\partial \tilde{H}}{\partial \tau}\right) \qquad (5)$$

and the appropriate boundary conditions according to equation (3) are

$$\tilde{P}(0, Y, \tau) = \tilde{P}(1, Y, \tau) = \tilde{P}(X, 0, \tau) = \tilde{P}(X, b/a, \tau) = 0. \qquad (6)$$

The thickness of the film under small harmonic motion could be represented by

$$H = 1 + \frac{a}{h_0}\left(X - \frac{1}{2}\right)\Theta \sin(\tau) \qquad \text{for} \qquad 0 \leqslant X \leqslant 1 \qquad (7)$$

hence

$$\tilde{H} = \left(X - \frac{1}{2}\right)\sin(\tau) \qquad \text{and} \qquad \delta = \frac{a\Theta}{h_0}. \qquad (8)$$

A small rotational motion of the mirror may suggest that the pressure variation relative to the ambient pressure is considerably smaller than the variations in the thickness of the film relative to the average thickness, meaning that $\tilde{P} \ll \tilde{H}$. Under such an assumption and since both the gap and the pressure vary in time at the same frequency, it seems logical to assume that $\partial\tilde{P}/\partial\tau \ll \partial\tilde{H}/\partial\tau$, and equation (5) can be degenerated into a Poisson equation of the form:

$$\frac{\partial^2\tilde{P}}{\partial X^2} + \frac{\partial^2\tilde{P}}{\partial Y^2} = \sigma\frac{\partial\tilde{H}}{\partial\tau} = \sigma\left(X - \frac{1}{2}\right)\cos(\tau) = f(X,\tau). \quad (9)$$

The above equation holds for small squeeze numbers where the flow could be considered incompressible and the film behaves as a viscous damper. Moreover, when dealing with large squeeze numbers, not only does the assumption made for deriving equation (9) not hold, but also the linearized Reynolds equation in equation (5) is no longer adequate. At large squeeze numbers, the spring-like behavior of the film is nonlinear and an additional levitation force is excreted [11, 7], influencing the system dynamics. Pan *et al* [6] have first found a solution for equation (5) and then neglected from it the torque generated by the air spring effect, while equation (9) actually neglects in the governing equation the term related with the spring effect and restrains the pressure in the film to be proportional to $\dot{\theta}$ only. In the practical sense, the solution of equation (9) for any arbitrary function describing the clearance $f(X, Y, \tau)$ could be easily obtained compared with that involved with equation (5). A convenient method for solving equation (9) is by employing the Green function technique in rectangular coordinates for which the solution for the pressure fluctuations takes the form

$$\tilde{P}(X,Y,\tau) = \int_0^{b/a}\int_0^1 f(\xi,\eta,\tau)G(X,Y,\xi,\eta)\,\mathrm{d}\xi\,\mathrm{d}\eta, \quad (10)$$

where the Green function for the Poisson equation is [13]

$$G(X,Y,\xi,\eta) = -\frac{4a}{b}\sum_{n=1,2\ldots}^{\infty}\sum_{m=1,2\ldots}^{\infty} \times \frac{\sin(n\pi X)\sin(n\pi\xi)\sin\left(\frac{m\pi a}{b}Y\right)\sin\left(\frac{m\pi a}{b}\eta\right)}{(n\pi)^2 + \left(\frac{m\pi a}{b}\right)^2}. \quad (11)$$

Substituting equation (11) into equation (10), integrating respectively and simplifying the terms in the double series summation, results in the expression for the pressure distribution as a function of time and space:

$$\tilde{P}(X,Y,\tau) = \frac{8\sigma}{\pi^2}\cos(\tau)\sum_{n=1,2\ldots}^{\infty}\sum_{m=1,2\ldots}^{\infty}\frac{1}{2n(2m-1)} \times \frac{\sin(2n\pi X)\sin\left((2m-1)\pi\frac{a}{b}Y\right)}{(2n\pi)^2 + \left((2m-1)\pi\frac{a}{b}\right)^2}. \quad (12)$$

Justifying the assumption of neglecting the contribution of the pressure fluctuation in time to the pressure spatial distribution can be done by considering the following typical physical dimensions of a micro torsion mirror in MKS units:

$$\begin{array}{lll} a = 500\times10^{-6}, & b = 500\times10^{-6}, & c = 30\times10^{-6}, \\ h_0 = 20\times10^{-6}, & p_0 = 1\times10^{5}, & \mu = 1.8\times10^{-5}, \\ \omega = 2\pi\times15\,000, & \Theta = 10^{-3}\ \text{rad}. & \end{array} \quad (13)$$

Under such conditions, the analytical results obtained by equation (12) confirm that indeed $\mathrm{Max}(\tilde{P}) = 0.000\,9343$ is significantly smaller than $\mathrm{Max}(\tilde{H}) = 0.5$.

The torque acting on the mirror, excreted by the pressure in the film, is

$$T = \int_0^{b/a}\int_0^1 (P(X,Y,\tau) - 1)\left(X - \frac{1}{2}\right)\mathrm{d}X\,\mathrm{d}Y = \int_0^{b/a}\int_0^1 \delta\tilde{P}(X,Y,\tau)\left(X - \frac{1}{2}\right)\mathrm{d}X\,\mathrm{d}Y \quad (14)$$

by defining

$$\Delta_{nm} = \sum_{n=1,2\ldots}^{\infty}\sum_{m=1,2\ldots}^{\infty}\frac{1}{(2n)^2(2m-1)^2} \times \frac{1}{(2n\pi)^2 + \left((2m-1)\pi\frac{a}{b}\right)^2} \quad (15)$$

and the dimensional expression for the damping torque is given as

$$M_\mathrm{D} = a^3 p_0 T = -\frac{192\Theta b a^5\omega\mu}{\pi^4 h_0^3}\Delta_{nm}\cos(\omega t). \quad (16)$$

2.1. The equivalent damping coefficient

The equation of motion of a rigid tilting mirror can be described by the one degree of freedom second-order linear differential equation:

$$I_\mathrm{y}\frac{\mathrm{d}^2\theta}{\mathrm{d}t^2} + D\frac{\mathrm{d}\theta}{\mathrm{d}t} + K\theta = M_\mathrm{E} + M_\mathrm{D}, \quad (17)$$

where I_y, D and K are the mass moment of inertia, the damping coefficient and the stiffness of the device, respectively. The external actuation moment applied to the system is designated by M_E. Assuming a harmonic rotational motion of the form $\theta = \Theta\sin(\omega t)$, substituting it into equation (17) and balancing the harmonic terms result in the expression of the form $D\dot{\theta} = M_\mathrm{D}$. The damping coefficient for a rectangular tilt mirror under the condition where the gas can be considered as a continuous medium is therefore

$$D = \frac{192ba^5\mu}{\pi^4 h_0^3}\Delta_{nm}. \quad (18)$$

It appears that the damping coefficient is independent of both the ambient pressure and the excitation frequency. As indicated by Pan *et al* [6], the independence of the damping coefficient on the excitation frequency enables the use of superposition of the Fourier sine series terms. The independence of the damping coefficient on the ambient pressure requires, in rare air conditions, the utilization of 'effective coefficient of viscosity' to artificially create a pressure dependence. Inspecting equation (49) in Pan *et al* [6] reveals that as long as $\sigma^2 \ll \pi^2$ (as in the present case), neglecting σ^2 is permissible and the damping coefficient is reduced identically to equation (18). For example, the squeeze number obtained under the typical operating conditions given in equation (13) is $\sigma = 0.127$. The damping ratio ζ is defined as

$$\zeta = \frac{D}{2I_\mathrm{y}\omega_\mathrm{n}}, \qquad I_\mathrm{y} = \rho_\mathrm{s}abc\frac{(a^2+c^2)}{12}, \quad (19)$$

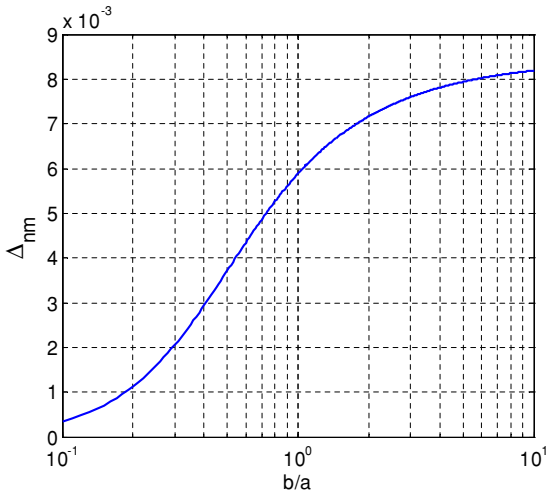

Figure 2. The converged values of the double series Δ_{nm} as a function of b/a.

where ω_n is the natural frequency of the mirror first tilting mode ($\zeta^2 \ll 1$). Hence, the damping ratio is expressed by

$$\zeta = \frac{1152a^4\mu}{\pi^4 h_0^3 \rho_s c(a^2+c^2)\omega_n}\Delta_{nm} \tag{20}$$

for cases where $c \ll a$, the damping ratio could be further simplified and the quality factor takes the form

$$Q_{SF} = \frac{1}{2\zeta} = \frac{h_0^3\rho_s c\omega_n \pi^4}{2304a^2\mu\Delta_{nm}}. \tag{21}$$

Figure 2 shows the converged values of the double series Δ_{nm} as a function of b/a. Clearly, the damping ratio decreases with the decreases of the ratio b/a, since the effective squeezing area is being reduced. For a square torsion mirror ($a = b$) the double series summation converges to $\Delta_{nm} = 5.886 \times 10^{-3}$.

2.2. *Effective coefficient of viscosity*

The approach of using effective coefficient of viscosity suggests that the squeeze-film equations remain effective in rare air conditions. The dependence on the pressure is implemented via an artificial viscosity coefficient as approximated by Veijola *et al* [1]

$$\mu = \frac{\mu_0}{1 + 9.658Kn^{1.159}} \tag{22}$$

or alternatively, utilizing the empirical equation given by Li and Hughes [2]:

$$\mu = \frac{\mu_0}{1 + 6.8636Kn^{0.9906}}. \tag{23}$$

The Knudsen number Kn determines the degree of rarefaction and the validity of the continuum model. It is the ratio of the free mean path of the gas molecules to the characteristic length of the flow.

$$Kn = \frac{\lambda}{L_c} = \frac{k_B T}{\sqrt{2}\pi d_{gas}^2 P L_c}, \tag{24}$$

where $k_B = 1.380\,658 \times 10^{-23}\,\mathrm{J\,K^{-1}}$ is Boltzmann's constant, T is the temperature (K), L_c is the characteristic length of the flow (in our case $L_c = h_0$), d_{gas} is the diameter of the gas molecule (for nitrogen $d_{gas} = 3.8 \times 10^{-10}$ m) and P stands for the gas pressure in Pascal units.

3. Free molecules model

The molecular model proposed by Christian [3] derives the damping force on an oscillating plate by calculating the momentum transfer rate from the vibrating plate to the surrounding air due to collisions of molecules with the plate. But this model does not consider the effect of a nearby wall; hence it is adequate for isolated vibrating plates. Bao *et al* [4] presented a molecular model based on energy transfer rather than momentum transfer. Bao has shown that for an isolated vibrating plate, the quality factor obtained by both approaches is identical. However, for an oscillating plate near a wall, the quality factor obtained by the energy transfer model is about one order of magnitude smaller than that obtained by the Christian model. In deriving the energy transferred from the vibrating plate to the molecules, Bao *et al* [4] have assumed that the time required for a molecule to travel under the plate is much shorter than the oscillation time period of the plate. Therefore, the velocity gained or lost after each collision remains the same during its travel time. Additionally, under vibration amplitudes of the plate that are much smaller than the mean gap, Bao *et al* [4] considered the gap to be constant during the entire travel of a molecule. The expression for quality factor provided by Bao *et al* [4] is

$$Q_{FM} = (2\pi)^{\frac{3}{2}}\rho_s c\omega\left(\frac{h_0}{L}\right)\sqrt{\frac{RT}{M_m}}\frac{1}{p}, \tag{25}$$

where $R = 8.31\,\mathrm{J\,K^{-1}/mole}$ is the ideal gas constant, M_m is the gas molar mass (28.92 g/mole for air) and L is the peripheral length of the plate ($L = 2a + 2b$ for a rectangular plate). In order to utilize Bao's model, we chose to approximate the tilt motion of the mirror as two halves of the mirror vibrating out of phase normally to the wall with a vibration amplitude of $a\Theta/4h_0$. This approximation holds since the rotational motion is very small relative to the mean gap thickness.

The quality factor is defined as the ratio between the total energy of the system (e.g., maximum kinetic energy of the plate) and the averaged energy loss during the time the phase angle moves one radian at resonant frequency, which gives rise to $Q = 2\pi E/\Delta E$. The average energy loss is obtained by integrating the change in the gas molecules kinetic energy leaving the area underneath the plate over one cycle in time. Therefore, the time phase between the two vibrating halves of the plate does not play a role over a time period, and the average energy loss is equivalent to that of a full plate oscillating normally to the wall at the same frequency. However, the peripheral length of the two halves is larger than that of a full plate and should be rectified accordingly. The assumption of constant gap during the travel of the molecules under the plate holds since the dimensionless vibration amplitude is small, i.e. $a\Theta/4h_0 \ll 1$. Consequently, the approximated quality factor for a torsion mirror in rare air using free molecule model could be obtained by using equation (25) with the appropriate peripheral length: $L = 2a + 4b$.

4. Experiments and comparison

In this section, the experimental measurements that were performed on two dedicated micro-machined mirrors are presented. The two mirrors are similar in dimensions but

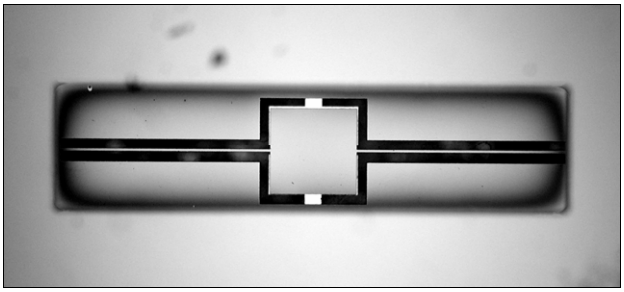

Figure 3. Upper view photograph of the torsion mirror.

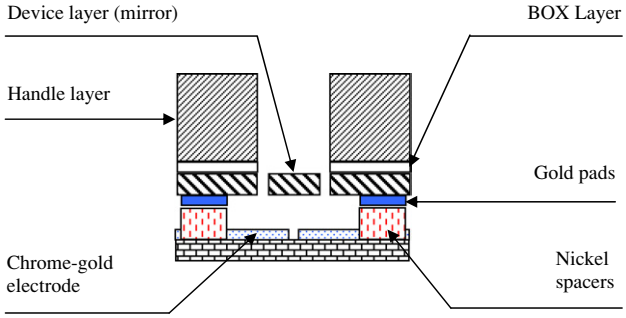

Figure 4. Schematic cross section of a diced micro-machined actuator.

have different gaps between the mirror and the electrodes thus having different damping characteristics. A brief description of the fabrication process of the micro device is followed by the description of the experimental configuration and the data analysis methods utilized for extracting the damping coefficient. Then, experimental results are examined and compared with the theoretical models

4.1. Fabrication process

The miniature resonating torsion mirror shown in figure 3 was designed according to an established process, consisting of a device die and a substrate die assembled together in a flip chip process [14, 15]. A SOI wafer consisting of a 30 μm device layer, a 350 μm handle layer and a 2 μm BOX layer was micro-machined by the following four main steps: (1) 2000 Å thick gold pads were deposited on the device layer for assembly purposes and served as electrical connections to the mirror. (2) A DRIE process on the handle side was used in order to free the mirror system from the handle layer and to enable optical access to the mirror. (3) Etching of the oxide layer is used to free the structure from the oxide layer. (4) A DRIE process on the device side is used in order to free the mirror system from the device layer thus completing its mechanical release and enabling it to vibrate freely.

The fabrication of the substrate consisted of a deposition of 2000 Å thick nickel–chrome–gold electrodes; this layer was used both for the electrostatic actuation of the mirror and also as a seed layer for the nickel electroplating, implemented in order to create a highly conductive spacer. This spacer allowed determining the gap between the electrodes and the mirror. The dimensions of the mirror seen in figure 3 are $500 \times 500 \times 30$ μm^3 and the dimensions of each torsion beam are $1195 \times 15 \times 30$ μm^3. The blurry rectangular shape seen around the mirror is the shade created by the handle layer. Figure 4 shows a schematic cross section of a diced micro-machined system, presenting the final configuration of the components.

In this work, the experiments were conducted on two different mirrors, having similar dimensions in terms of surface area and inertial moment, but having different gaps between the mirror and the actuation electrodes. The nominal values of the physical parameters of the two mirrors (referred to as mirror 1 and mirror 2) are summarized in table 1. The dimensions a and b are basically mask dependent so a ± 1 μm is estimated and the mirror's thickness c is the wafer's device thickness (see figure 4) with a ± 1 μm manufacturing tolerance error.

Table 1. Physical parameters of the two mirrors.

	Mirror 1	Mirror 2
a, b (μm)	500 ± 1	500 ± 1
z (μm)	58 ± 1	43 ± 1
c (μm)	30 ± 1	30 ± 1
f_n (Hz)	$13\,092.56 \pm 0.01$	$12\,824.87 \pm 0.01$
ΔQ_{SF}	13%	30%
ΔQ_{FM}	4%	9%

A sensitivity analysis reveals, as one may expect, that the damping coefficient value is dominated by the level of the mirror proximity to the electrodes (h_0). Once the micro-resonator system was assembled, the distance between the reflecting (upper) side of the mirror and the exposed surface of the actuating electrodes was measured by optical means using a microscope. Designating this dimension by z, the accuracy of the optical measurement was approximately $\Delta z = \pm 1$ μm. Additionally, the thickness of the device layer imbedded in the SOI wafer had a possible manufacturing tolerance error of about $\Delta c = \pm 1$ μm. Consequently, the gap clearance is implicitly determined by $h_0 = z - c$, and the uncertainty in the quality factor due to the uncertainty in the above two independent geometrical dimensions could be approximated by

$$\Delta Q = \sqrt{\left(\frac{\partial Q}{\partial c}\Delta c\right)^2 + \left(\frac{\partial Q}{\partial z}\Delta z\right)^2}. \tag{26}$$

The percentage of uncertainties in the quality factor calculated according to the squeeze-film model (ΔQ_{SF}), based on equation (21), and according to the free molecules model (ΔQ_{FM}), based on equation (25), are summarized in table 1. For a given tolerance in the systems' geometrical dimensions, the smaller the clearance between the mirror and the electrodes, the higher the possible error in estimating the quality factor.

4.2. Experimental set-up and procedures

The experimental set-up consisted of a laser vibration and displacement sensor, a multi-channel, 16-bit data-acquisition system sampling at a rate of 200 kHz and a custom-made vacuum chamber. Passing through an optical microscope and a transparent window in the chamber, the measuring laser beam is being reduced to a diameter of 5 μM. The laser beam was located near the edge of the mirror far from the rotation axis, thus attaining maximum sensitivity in the rotational mode of motion. On each of the two electrodes implanted on the

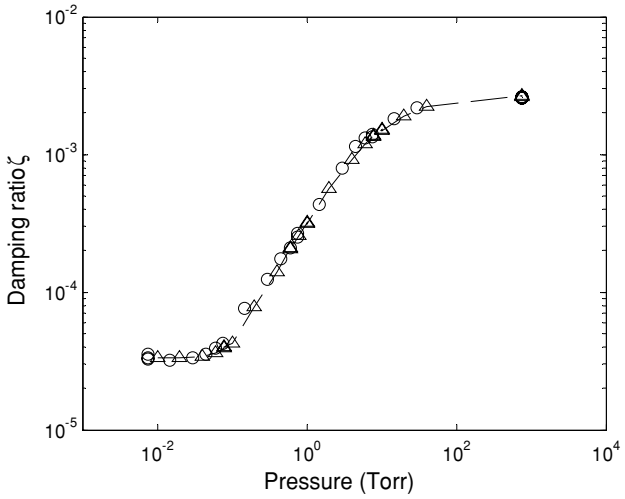

Figure 5. Experimental results of the damping ratio in mirror 1 as a function of pressure: (circles) based on steady state, stepped-sine measurements, (triangles) based on transient response.

substrate, an equal dc voltage with opposite potentials was applied. The device layer, which the torsion mirror is part of, was subjected to an ac voltage at the excitation frequency.

Two different methods for extracting the damping ratio of the system from the experimental data were employed. In one method, a sinusoidal excitation signal is injected to the system and the steady-state response is curve fitted. This process is repeated for a large number of discrete frequencies, one at a time, and the amplitude and phase of the response are recorded. Good accuracy and frequency resolution were achieved with this method, as frequencies could be spaced 1 mHz apart in frequency ranges where the amplitude varies sharply (i.e. resonance with high Q factor). To the measured frequency response, a parametric transfer function of the form

$$H(s) = \frac{b_2 s^2 + b_1 s + b_0}{s^2 + a_1 s + a_0} \tag{27}$$

was fitted according to Levi [16], where $s = \mathrm{i}\omega$. Finding the polynomial coefficients of the denominator yields the damping coefficient.

The second method that was utilized is based on the decay rate of a transient response using the Hilbert transform. In this case, the mirror was excited by a square wave at low frequency and the measured velocity, $v(t)$, at each transient has the form

$$v(t) = A\,\mathrm{e}^{-\zeta\omega_\mathrm{n}t}\sin\left(\sqrt{1-\zeta^2}\omega_\mathrm{n}t + \phi\right), \tag{28}$$

where $\zeta, \omega_\mathrm{n}, \phi, A$ are the damping ratio, natural frequency, phase delay and amplitude, respectively. The measurements of the mirrors' transient displacement were triggered by the upgoing part of the square wave and several response measurements were synchronously averaged in the time domain to remove the non-synchronous frequencies. The envelope of the time-averaged response, $A\,\mathrm{e}^{-\zeta\omega_\mathrm{n}t}$, was then extracted by utilizing the Hilbert transform [17], and the damping ratio was computed by fitting a decaying exponential to this curve. A more detailed explanation of the two damping extraction methods together with samples of the experimental data is provided in the appendix.

Figure 5 presents the damping ratio ζ of mirror 1 estimated from the measured response as a function of vacuum level. A small rotational amplitude was assured by not allowing the maximal rotational amplitude to exceed 0.01 rad. The circles on figure 5 designate the results obtained by the curve fitting method and the triangles designate the results obtained from the transient response. The good agreement between the two different methods enhances the confidence in the experimental results, and could serve as a reliable basis to assess the theoretical models.

4.3. Experimental results

A series of measurements was conducted on the two micro-machined torsion mirrors, manufactured in the same fabrication process having similar dimensions and properties but with different clearances between the mirror and the electrodes, as detailed in table 1. The quality factors (Q) extracted from the experimental data were compared with the theoretical models outlined in the first two sections of this work.

The quality factor based on the squeeze-film model was obtained by substituting the equivalent viscosity given in equation (22) and in equation (23) together with equation (24) into the expression for the quality factor in equation (21). The quality factor based on the free molecules model was obtained directly from equation (25). Figure 6 presented the experimental results (squares) plotted together with the squeeze-film models based on the equivalent viscosity as suggested by Veijola (dotted curves) and by Li and Hughes (solid curves). The results obtained by the modified Bao's free molecule model are plotted as dashed lines in figure 6.

Keeping in mind the level of uncertainty described in section 4.1, figure 6 indicates a relatively good agreement between the theoretical models and the experimental results. Among the three models, the least adequate model for predicting the quality factor is the squeeze-film model based on the equivalent viscosity suggested by Veijola (dotted curves), which underestimates the gas damping at high vacuum levels. As expected, the free molecules model is suitable only for pressure regimes where the mean free path of the gas molecules is of the same or higher order as the characteristic length of the flow.

Examining the prediction obtained by Bao's model reveals that the agreement with the experimental results is better for mirror 1, where the nominal clearance is 28 μm, while for mirror 2, where the nominal clearance is smaller 13 μm, the quality factors are overestimated. This could be related to the assumption, made by Boa *et al* [4], of constant particle velocity while traveling in the gap. The assumption of constant particle velocity implies that the number of collisions is constant with no distinction between molecules that increase their velocity and molecules that decrease their velocity in each collision. The modified model provided by Hutcherson and Ye [5] does take into consideration that the number of collisions of molecules which gain velocity at each collision is larger than the number of collisions of molecules which lose velocity, and by doing so, reduces the underestimation of the energy gained by the gas molecules. As derived by Bao *et al* [4], the number of collisions while a molecule travels underneath the mirror is inversely proportional to the gap thickness (equation (6) in Hutcherson and Ye [5]). Hence, the larger

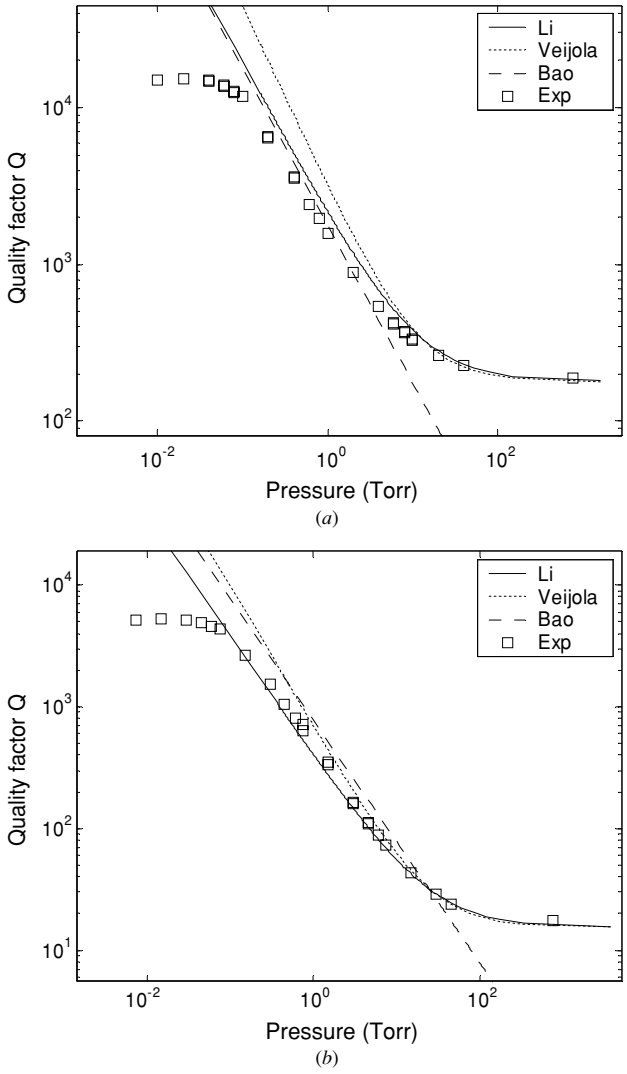

Figure 6. The experimental and theoretical results for the quality factor versus pressure for: (*a*) mirror 1, (*b*) mirror 2.

the gap between the mirror and the electrodes, the smaller the number of collisions, and consequently, the constant particle velocity assumption becomes more reasonable.

At a certain vacuum level, the gas damping becomes insignificant in comparison with other damping mechanisms such as the structural damping which is independent of the ambient pressure. Obviously, the damping models that are dealt with in this work and are compared in figure 6 do not consider such damping mechanisms. However, the experimental results may suggest that at vacuum levels higher than 10^{-1} Torr, the gas damping in micro-machined actuators is no longer the dominating damping mechanism and the damping becomes independent of the ambient pressure.

5. Conclusions

A theoretical and experimental study of the damping of micro torsion mirror in rarefied gas ambient has been performed. It has been shown that for small squeeze numbers, as in this case, the governing nonlinear Reynolds equation can be reduced to a Poisson equation, neglecting the rate of pressure fluctuations in time. Such a simplification allows obtaining analytical solutions to arbitrary functions of the film thickness in a straightforward manner (as long as the variations relative to the mean thickness are small). It has been concluded that the Bao's free molecule model can be adapted for the case of a torsion mirror by modifying the peripheral length appropriately. The experimental results of the damping ratio were obtained by utilizing two different methods, assuring the validity of the results. Comparison of the theoretical models with the experimental results has shown that the least suitable model is the one based on the equivalent viscosity suggested by Veijola *et al* [1]. The agreement of Bao's free molecule model with the measured data deteriorates as the clearance between the mirror and the electrodes decreases, possibly due to the inadequacy of the assumption of constant particle velocity. It appears that at vacuum levels above 10^{-1} Torr, the gas damping is no longer the dominating damping mechanism.

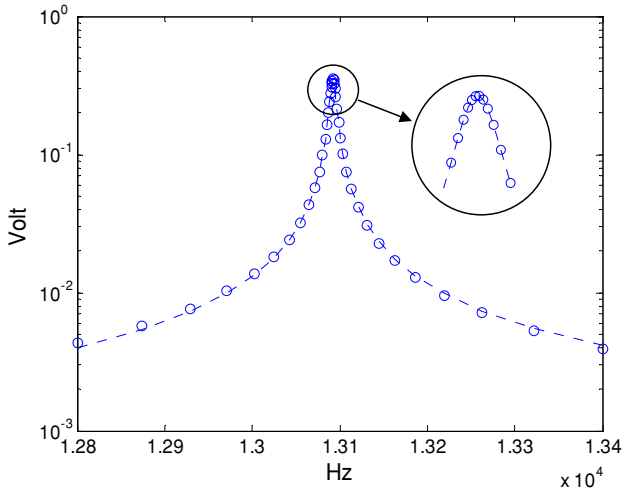

Figure A1. Measured frequency response of mirror 1, curve-fitted amplitude (circles) and fitted transfer function (dash-line). Here the ambient air pressure is 0.8 Torr and the damping ratio is $\zeta = 0.2655 \times 10^{-3}$.

Appendix

This appendix provides a short explanation on the damping extraction methods used in this work and presents samples of the obtained measurements. For comparison's sake, the mirrors' dynamic behavior under a specific ambient pressure is analyzed by the two methods showing the quality of the experimental measured data and the level of agreement with the fitted models.

Figure A1 presents the frequency response of the torsion mirror extracted from the mirrors' steady-state response to a sinusoidal excitation. Under the assumption of linear behavior, at each excitation frequency, the vibration amplitude amplification level (circles on figure A1) was obtained by curve fitting the measured laser's output signal with a harmonic function at the given excitation frequency. The curve fitting took into consideration possible offset or drift and was done by means of the least-squares method. At rarified ambient, the amplitude varies sharply near resonance (high

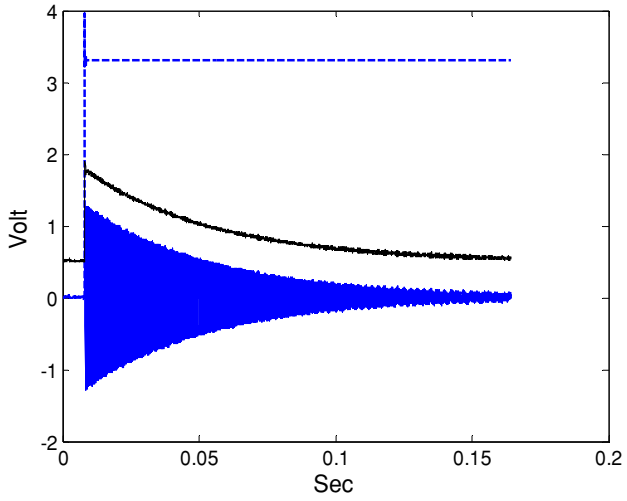

Figure A2. Time-averaged measured transient response of the torsion mirror (solid line) due to a square wave excitation at low frequency (dashed line). Here the ambient air pressure is 1 millibar and the damping ratio is $\zeta = 0.2553 \times 10^{-3}$.

Q factor); therefore, in order to achieve good accuracy and high frequency resolution, a signal generator able to space the frequencies up to 1 mHz apart served as the input excitation. In addition, a logarithmic stretching of the frequency range was applied to depict a wide band of the frequency response while keeping high clustering of samples close to resonance (as seen in figure A1).

Having the measured frequency response, a parametric continuous-time complex transfer function was fitted according to the method suggested by Levi [16]. This method converts magnitude and phase data into transfer functions in the form of numerator and denominator polynomials. The order of the polynomials, as seen in equation (27), was found to be sufficient for fitting the data in this work (dash-line in figure A1). Having the denominator polynomial coefficients of the transfer function allows calculating the damping ratio. In ambient air pressure of 0.8 Torr, the damping ratio of mirror 1 derived from the measured data shown in figure A1 is $\zeta = 0.2655 \times 10^{-3}$.

The second method that was utilized is based on curve fitting the decay rate of a transient response. Figure A2 presents the time-transient response of the torsion mirror (solid line) due to a square wave excitation at low frequency (1 Hz). The measurements of the transient response were triggered by the upgoing part of the square wave (dashed line on figure A2) and several response measurements were synchronously averaged in the time domain, removing non-synchronous frequencies and producing a curve according to equation (28). The envelope of the time-averaged response is then extracted by utilizing the Hilbert transform [17].

The instantaneous amplitude of the complex analytic signal determines the envelope of the real part. Creating an analytic signal in which the real part is the measured transient response and the imaginary part is the Hilbert transform allows us to obtain the logarithmic decay envelope of the transient response. This envelope is plotted in figure A2 and is intentionally shifted up by 0.5 V for presentation purposes only.

This method can provide an indication for the dependence of damping on the amplitude of vibration. For a system having a linear dynamic behavior, it is expected that on a logarithmic scale the envelope should appear as a straight line, indicating that the damping ratio does not depend on the vibration amplitude and is therefore constant. As the Hilbert transform is sensitive to noise, a curve was fitted only to data that belong to the beginning of the transient response where the ratio of noise to signal is relatively low. In ambient air pressure of 1 millibar (∼0.8 Torr) the damping ratio of mirror 1 derived from the measured data shown in figure A2 is $\zeta = 0.2553 \times 10^{-3}$. This damping ratio differs by less than 4% from that obtained by the steady-state response ($\zeta = 0.2655 \times 10^{-3}$). The good agreement between the two models gives high confidence in the validity of the data analysis.

References

[1] Veijola T, Kuisma H, Lahdenpera J and Ryhanen T 1955 Equivalent-circuit model of the squeezed gas film in a silicon accelerometer *Sensors Actuators* A **48** 239–48

[2] Li G and Hughes H 2000 Review of viscosity damping in micro-machined structures *Proc. SPIE* **4176** 30–46

[3] Christian R G 1966 The theory of oscillating-vane vacuum gauges *Vacuum* **16** 175–8

[4] Bao M, Yang H, Yin H and Sun Y 2002 Energy transfer model for squeeze-film air damping in low vacuum *J. Micromech. Microeng.* **12** 341–6

[5] Hutcherson S and Ye W 2004 On the squeeze-film damping of micro-resonators in the free-molecule regime *J. Micromech. Microeng.* **14** 1726–33

[6] Pan F, Kubby J, Peeters E, Tran A and Mukherjee S 1998 Squeeze film damping effect on the dynamic response of a MEMS torsion mirror *J. Micromech. Microeng.* **8** 200–8

[7] Minikes A, Bucher I and Haber S 2004 Levitation force induced by pressure radiation in gas squeeze films *J. Acoust. Soc. Am.* **116** 217–26

[8] Hao Z, Clark R, Hammer J, Whitley M and Wingfield B 2002 Modeling air-damping effect in bulk micromachined 2D tilt mirror *Sensors Actuators* A **102** 42–8

[9] Uchida N, Uchimaru K, Yonezawa M and Sekimura M 2000 Damping of micro electrostatic torsion mirror caused by air-film viscosity *13th Annual Int. Conf. on Micro Electro Mechanical Systems, MEMS 2000* pp 449–54

[10] Langlois W E 1962 Isothermal squeeze films *Q. Appl. Math.* **20** 131–50

[11] Salbu E O J 1964 Compressible squeeze films and squeeze bearings *J. Basic Eng.* **86** 355–66

[12] Blech J J 1983 On isothermal squeeze films *J. Lubr. Technol.* **105** 615–20

[13] Polyanin A D 2002 *Handbook of Linear Partial Differential Equations for Engineers and Scientists* (London: Chapman & Hall)

[14] Madou M J 2002 *Fundamentals of Microfabrication: The Science of Miniaturization* (Boca Raton, FL: CRC Press)

[15] Maluf N 2000 *Introduction to Microelectromechanical Systems Engineering* (Boston, MA: Artech House)

[16] Levi E C 1959 Complex-curve fitting *IRE Trans. Autom. Control* **4** 37–44

[17] Feldman M 2001 *Hilbert Transforms, Encyclopedia of Vibration* (New York: Academic) pp 642–8